

New photometry and astrometry of the isolated neutron star RX J0720.4-3125 using recent VLT/FORS observations*

Thomas Eisenbeiss^{1,**}, Christian Ginski¹, Markus M. Hohle^{1,2}, Valeri V. Hambaryan¹, Ralph Neuhäuser¹, and Tobias O. B. Schmidt¹

¹ Astrophysikalisches Institut und Universitäts-Sternwarte Jena, Friedrich-Schiller-Universität Jena, Schillergässchen 2-3, 07745 Jena

² Max Planck Institut für extraterrestrische Physik Garching, Giessenbachstrasse, 85738 Garching

The dates of receipt and acceptance should be inserted later

Key words Stars: neutron - Dense matter - Stars: imaging - Techniques: image processing - Stars: individual

Since the first optical detection of RX J0720.4-3125 various observations have been performed to determine astrometric and photometric data. We present the first detection of the isolated neutron star in the V Bessel filter to study the spectral energy distribution and derive a new astrometric position. At ESO Paranal we obtained very deep images with FORS 1 (three hours exposure time) of RX J0720.4-3125 in V Bessel filter in January 2008. We derive the visual magnitude by standard star aperture photometry. Using sophisticated resampling software we correct the images for field distortions. Then we derive an updated position and proper motion value by comparing its position with FORS 1 observations of December 2000. We calculate a visual magnitude of $V = 26.81 \pm 0.09$ mag, which is seven times in excess of what is expected from X-ray data, but consistent with the extant U, B and R data. Over about a seven year epoch difference we measured a proper motion of $\mu = 105.1 \pm 7.4$ mas yr⁻¹ towards $\theta = 296.951^\circ \pm 0.0063^\circ$ (NW), consistent with previous data.

© 2006 WILEY-VCH Verlag GmbH & Co. KGaA, Weinheim

1 Introduction

In deep optical follow-up observations of bright X-ray sources from the ROSAT mission (Voges et al. 1999) seven thermal emitting isolated neutron stars (INS), exhibiting no radio emission, have been discovered so far (see Haberl 2004 2007; van Kerkwijk & Kaplan 2007 for recent reviews).

After the first optical detection of the brightest one, RX J1856.4-3754 (Walter, Wolk, & Neuhäuser 1996), Haberl et al. (1997) found the second brightest INS RX J0720.4-3125. It was detected in the optical B and R band by Kulkarni & van Kerkwijk (1998). Using deep observations Motch, Zavlin, & Haberl (2003) derived the proper motion of RX J0720.4-3125 and measured the B magnitude with VLT/FORS 1. Later Kaplan, van Kerkwijk, & Anderson (2007) measured the distance of RX J0720.4-3125 (~ 360 pc) and updated the proper motion using Hubble Space Telescope (HST) observations.

Comparing blackbody fits derived from X-Ray observations with the flux measured in the optical/UV wavelength (Motch et al. 2003) shows that RX J0720.4-3125 exceeds its expected optical/UV flux by about an order of magnitude (Hambaryan et al. 2009). Furthermore Haberl et al. (2006) detected variations in the X-ray flux. The origin of these

variations is still controversial (Hohle et al. 2009; Kaplan et al. 2007).

In this paper we measure the V magnitude for the first time and update the proper motion and absolute position.

In Section 2 we discuss the observations and data reduction. Sections 3 and 4 addresses the photometry. In Section 5 we discuss how our newly derived V magnitude fits with the investigations of earlier work. Section 6 is dedicated to our astrometric investigations and in Section 7 we summarize our results.

2 Observations and Data reduction

In January of 2008 we observed RX J0720.4-3125 for about three hours exposure time at ESO Paranal observatory with the Focal Reducer/low dispersion Spectrograph (FORS 1, Appenzeller et al. 1998), installed in Unit Telescope Kueyen of the Very Large Telescope (VLT). Observations were carried out in the V Bessel filter. We used a pixel scale of $0.125''/\text{pixel}$ which leads to a field of view of $4.2' \times 4.2'$. 13 single exposures of 900 s were taken over 1.5 nights.

For astrometric calibration we observed the globular cluster 47-Tuc with a pointing at $\alpha = 00^h 22^m 29.3^s$ and $\delta = -71^d 59' 54.3''$. The observations are summarized in Table 1. The image of the RX J0720.4-3125 field is shown in Fig. 1.

All images were flat fielded and bias subtracted. Since FORS 1 got a new detector in 2007 we were restricted to absolute world coordinates for astrometric comparison to

* Based on observations made with ESO Telescopes at the Paranal Observatory under programme ID 080.D-0135(A). Based on observations with XMM-Newton, an ESA Science Mission with instruments and contributions directly funded by ESA Member states and the USA (NASA).

** Corresponding author: e-mail: eisen@astro.uni-jena.de

Table 1 Observation log

| Date | Instrument telescope | Filter | Exp s | Pixel (") | Seeing (") | Target |
|-------------------------|----------------------|----------|------------------|-----------|------------|---------------------|
| 12 Jan. 2008 | FORS1/VLT-UT1 | V Bessel | $8.1 \cdot 10^3$ | 0.125 | 1.1 | RX J0720.4-3125 |
| 13 Jan. 2008 | FORS1/VLT-UT1 | V Bessel | $3.6 \cdot 10^3$ | 0.125 | 0.8 | RX J0720.4-3125 |
| 12 Jan. 2008 00:42 (UT) | FORS1/VLT-UT1 | V Bessel | $4 \cdot 10$ | 0.125 | 1.6 | 47-Tuc |
| 12 Jan. 2008 00:47 (UT) | FORS1/VLT-UT1 | V Bessel | 12 | 0.125 | 1.6 | Landolt field SA 98 |
| 12 Jan. 2008 04:48 (UT) | FORS1/VLT-UT1 | V Bessel | 5 | 0.125 | 1.1 | Landolt field SA 98 |

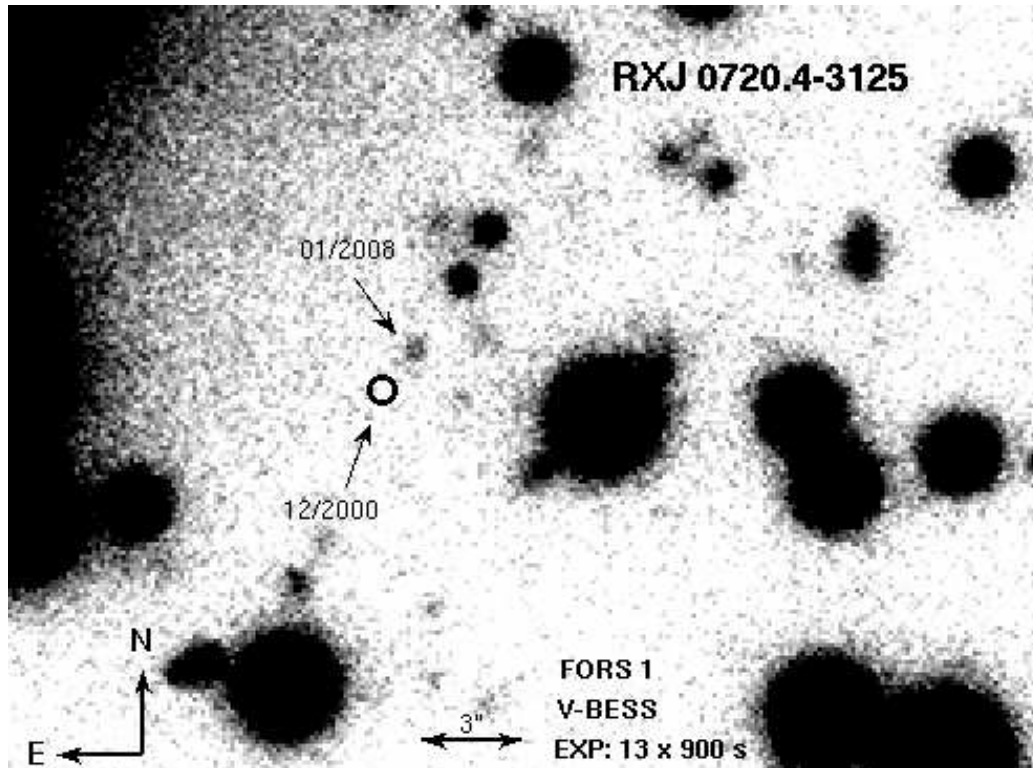


Fig. 1 Co-added V band images obtained with FORS 1 on Kueyen in January 2008. The circle shows the position of RX J0720.4-3125 as measured in the FORS 1 image of December 2000 (Motch et al. 2003). The arrow labeled 01/2008 points to our detected position of RX J0720.4-3125.

earlier observations. Furthermore the new chip is divided in two parts which limits the number of reference stars on each part. In order to derive an accurate astrometric solution we observed the globular cluster 47-Tuc at four dither positions. Based on the ESO fits header we derived image, as well as world coordinates of each object in the images with the *Source Extractor* (SE, Bertin & Arnouts 1996). These object catalogs are fitted with reference to the two micron all sky survey catalog (2MASS, Cutri et al. 2003), provided by the ViZiR database (Ochsenbein, Bauer, & Marcout 2000). After the WCS frame is calibrated in that way a fifth order polynomial is fitted to the data. This χ^2 -algorithm corrects the remaining field distortions. We used the software *SCAMP*¹ (Bertin 2006) for these calculations. *SCAMP* stores the calibration information (WCS transformation as well as field distortion coefficients) in an external header for each image. We extracted the field distortion coefficients,

¹ Software for Calibrating AstroMetry and Photometry

we derived calibrating the 47-Tuc images and used them as input for the calibration procedure of the RX J0720.4-3125 images, which is done by *SCAMP* as well in the same way. Similar, but directly without using a calibration cluster the RX J0720.4-3125 images of the year 2000 observed by Motch et al. (2003) were calibrated. The field distortion map of this calibration is shown as an example in Fig. 2.

Another software called *SWarp* (Bertin et al. 2002) uses the external headers produced by *SCAMP* to align, resample, and co-add the images. A mesh based background subtraction is applied during co-addition and the two parts of the chip are stitched together. This is illustrated in Fig. 3.

Typically the semi major axis of the error ellipse of 2MASS does not exceed 0.3 arcsec. The statistical errors of the source detection procedure are much smaller. *SCAMP* preselects unambiguous, well exposed sources for the fitting and treats the uncertainties in a χ^2 sense. Nevertheless it is unnecessary to treat each error source individually. The

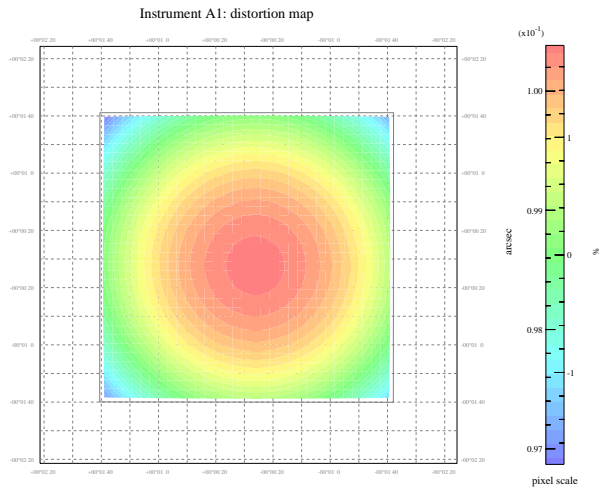


Fig. 2 Field distortion map of FORS 1 detector in December 2000. Color coding goes from red (middle in the image and top of the scale) through yellow and green to blue (corners of the image and bottom of the scale.)

resulting measurement plus calibration error is calculated in a statistical way as described in Section 6.

3 Photometry for January 12th, 2008

To flux-calibrate the image we observed the Landolt standard star field SA98 (Landolt 1992) in the first night. Since the standards were taken only in the first night we used the nine images of RX J0720.4-3125 taken in the first night for standard star photometry. We co-added them in the same way as described above, but only the upper part of the chip was used this time to avoid possible systematic photometry errors as they may happen while equalizing the background of the two parts of the FORS 1 detector. In the upper half of the chip only the two standard stars 98 556 and 98 557 were observed at airmasses 1.656 and 1.112, respectively, (Fig. 4). During data analysis it turned out, that there are faint objects nearby. Using the Landolt magnitudes for the stars and the given errors we first calculated the difference between the two magnitudes of the stars as measured by Landolt and by us assuming that

$$V_{556, \text{Land}} - V_{557, \text{Land}} \approx V_{556, \text{inst}} - V_{557, \text{inst}},$$

where V_{inst} are our instrumental magnitudes. Our measurements show that the stars marked as c1 and c2 in Fig. 4 were included in the aperture of Landolt (1992) so we took them into account accordingly. Aperture photometry is done using the DAOPHOT package (Stetson 1987).

We measured the instrumental magnitudes of both standard stars in each field and calculated the zero point correction c and the first order extinction coefficient k . Taking into account all sources of error, which is the 3σ error of the instrumental magnitude, the error of the Landolt magnitudes and the difference between the values by using the different

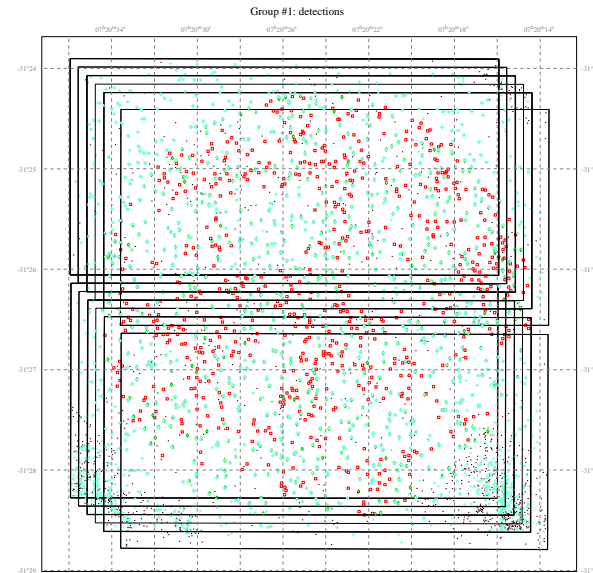


Fig. 3 Illustration how SCAMP co-added the 13 FORS 1 images (two parts of the chip). We used a dither pattern of four positions to avoid bad pixels. Diamonds and pluses symbolize objects found in each, or at least some of the images and used for calculation of the astrometric solution while squares symbolize objects not used for calibration. The rectangles illustrate the chip shape and the relative position.

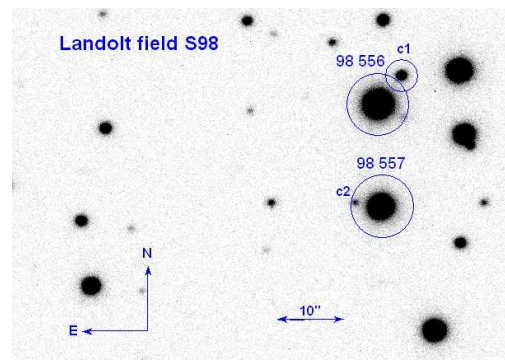


Fig. 4 VLT/FORS1 image of the Landolt standard stars 98 556 and 98 557. There are two objects close to the standard stars, marked as c1 and c2, which contribute flux to the standard magnitude measured by Landolt (1992) so we measured the flux of these objects as well and took their contribution into account.

standard stars we derive

$$c = (-21.0832 \pm 0.0017) \text{ mag and} \\ k = (0.1562 \pm 0.0058) \text{ mag.}$$

Since these quantities are derived using two different stars, their uncertainties include an estimation of the error, which is made neglecting the color term.

The most pronounced error source comes from the faint INS magnitude measurement itself. Fig. 1 shows the rim of

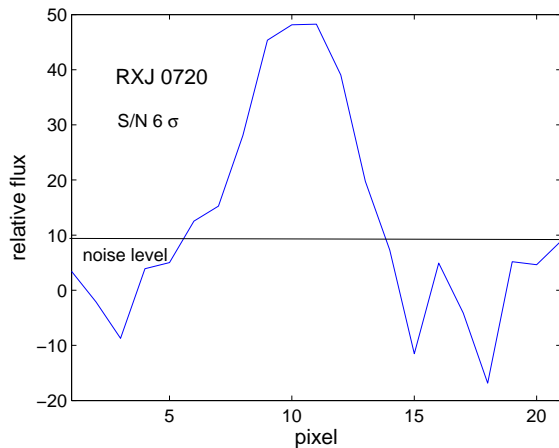


Fig. 5 Projection of the detection of RX J0720.4-3125 . The neutron star is detected with $\sim 6\sigma$.

an association of bright O-stars to the left of RX J0720.4-3125 . In our deep exposures these stars influence the background, so we had to choose an aperture smaller than that in the standard star image to deal with this problem. The INS is detected at $\sim 6\sigma$. Because of the faintness of the source only the top of the PSF has a higher count rate than the background hence, for the INS a smaller aperture than for the reference stars is possible (Fig. 5). We investigated the magnitude - aperture dependence of this faint source and concluded from our measurements and Fig. 5 that an aperture radius of seven pixels is sufficient.

Using the uncertainties of c and k and taking the variation of the airmass ($Y_{\text{NS}} = 1.028 \pm 0.019$) during observation into account we finally derive the V magnitude of RX J0720.4-3125 to be

$$V = (26.88 \pm 0.15) \text{ mag, for Jan 12th, 2008.}$$

4 Photometry for January 13th, 2008

Four images were taken in the second night under much better seeing conditions than the first night. Since the most pronounced source of error in the absolute photometry was the measurement of the faint INSs magnitude itself, we decided to use these images too, even though no official photometric standards were taken that night. We co-added the images as before and explained in Section 2. In addition we were using the *SE* to apply a background subtraction. The *SE* uses a mesh based background algorithm with a mesh size of 64 pixels. In the resulting image we identified three reference stars near RX J0720.4-3125 with known V-band magnitudes (Motch & Haberl 1998 and Fig. 6).

We used an aperture of 15 pixel radius for the reference stars, given by the full width at half maximum (FWHM) size of ≈ 4.5 pixel. For the INS we determined the object's size. It turned out that the PSF of the INS vanishes below the background at a radius of less than five pixels, so we chose the aperture radius accordingly. Furthermore we

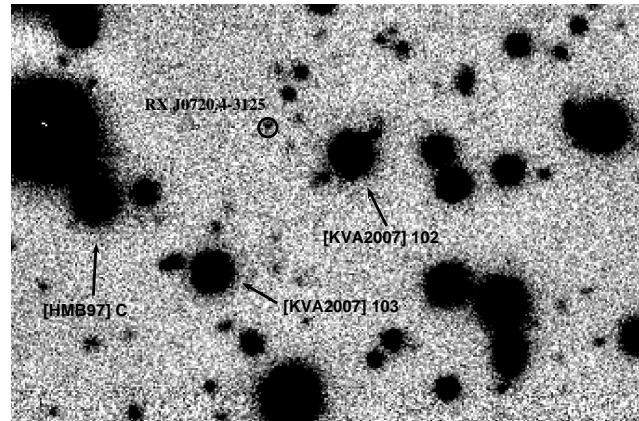


Fig. 6 Co-added and background subtracted image used for relative photometry. The reference stars used are named and marked by arrows. Motch & Haberl (1998) measured their V magnitude with an accuracy of 0.05 mag. The INS is marked and the aperture radius (5 pixel, circle) is shown.

chose smaller inner and outer sky radii compared to the reference stars to prevent the neighboring stars from falling into the background annulus.

The difference of the instrumental and the apparent magnitudes for each reference star is calculated. The mean of this difference gives again the detector zero point, so this the magnitude of RX J0720.4-3125 is determined to be

$$V = (26.81 \pm 0.09) \text{ mag, for Jan 13th, 2008}$$

which is fully consistent with our other measurement.

Note, that if the small aperture would have caused any loss of flux the magnitude of the INS would be larger instead. Since the error bar is smaller we use the relative value in the following discussion.

5 The Spectral Energy Distribution of RX J0720.4-3125

The visual magnitude of RX J0720.4-3125 is consistent with an optical excess about an order of magnitude larger than the expected flux extrapolated from the X-ray spectra first reported in Kulkarni & van Kerkwijk (1998) and studied in detail by Kaplan et al. (2003). However, the origin of this enigmatic property as well as its relation to the X-ray variations is still unknown and a matter of debate, see Haberl (2007) and Haberl et al. (2006) for a review about the INSs and RX J0720.4-3125 in particular. It might be possible that the emitting area of the soft X-ray radiation is not strictly connected to the source of optical/UV photons (Hambaryan et al. 2009). Trümper (2005); Turolla, Zane & Drake (2004); Zane, Turolla & Page (2007); Zane, Turolla & Drake (2004) and references therein discuss alternative explanations of the optical excess. The radius of the X-Ray emitting area is ≈ 4.5 km (Haberl et al. 2006), normalized to a distance of 300pc.

Table 2 Optical, ground based observations of RX J0720.4-3125. Only measurements of ground based observations are shown, in contrast to Fig. 7, where HST observations from Kaplan et al. (2003) are included. Other references are given in the table.

| Filter | Mag | Flux density | λ_{cent} | Flux | Reference |
|--------|--------------------|---|-------------------------|--|-----------------------------------|
| | | $[\text{W/m}^2/\text{Hz}] \cdot 10^{-34}$ | $[\text{\AA}]$ | $[\text{erg s}^{-1} \text{cm}^{-2}] \cdot 10^{16}$ | |
| U | 25.68 ± 0.17 | $9.75^{+1.65}_{-1.42}$ | 3600 | $8.13^{+1.38}_{-1.18}$ | Motch et al. 2003 |
| B | 26.58 ± 0.25 | $9.64^{+2.46}_{-1.98}$ | 4300 | $6.73^{+1.72}_{-1.38}$ | Motch et al. 2003 |
| | 26.79 ± 0.20 | $7.94^{+1.61}_{-1.33}$ | 4300 | $5.54^{+1.12}_{-0.93}$ | Motch et al. 2003 |
| | 26.44 ± 0.15 | $11.00^{+1.60}_{-1.45}$ | 4300 | $7.67^{+1.12}_{-1.01}$ | Motch et al. 2003 |
| | 26.787 ± 0.040 | $7.96^{+0.30}_{-0.28}$ | 4300 | $5.55^{+0.21}_{-0.20}$ | Motch et al. 2003 |
| | 26.620 ± 0.050 | $9.29^{+0.44}_{-0.42}$ | 4300 | $6.48^{+0.31}_{-0.29}$ | Motch et al. 2003 |
| V | 26.81 ± 0.09 | $6.69^{+0.99}_{-0.86}$ | 5500 | $3.65^{+0.54}_{-0.47}$ | this paper |
| R | 26.9 ± 0.3 | $5.11^{+1.63}_{-1.23}$ | 7000 | $2.19^{+0.70}_{-0.53}$ | Kulkarni & van Kerkwijk 1998 |
| H | $>23.07 \pm 0.11$ | $< 7.75^{+0.80}_{-0.72}$ | 16500 | $< 12.29^{+1.32}_{-1.12}$ | Posselt et al. 2009 (upper limit) |

For comparison to other optical/UV magnitudes we show in Fig. 7 the flux expected from a black body model (XMM-Newton EPIC-pn). The effective temperature of RX J0720.4-3125 is changing on time scales of years, see Hohle et al. (2009) and Haberl et al. (2006).

We plot in Fig. 7 the spectra obtained with XMM-Newton EPIC-pn with lowest (orbit 0078) and highest (orbit 0815) temperatures ($86.5 \pm 0.4 \text{ eV}$ and $94.6 \pm 0.5 \text{ eV}$, respectively) measured yet. The values were obtained by fitting the spectra with standard software *xspec12* (Dorman, Arnaud, & Gordon 2003) in the energy range of 0.16-1.5 keV by applying a black body model with additive gaussian absorption line (line energy = $301 \pm 3 \text{ eV}$, $\sigma = 77 \pm 2 \text{ eV}$) with absorption due to the ISM ($N_H = 1.04 \pm 0.02 \cdot 10^{20} \text{ cm}^{-2}$), see Hohle et al. (2009) for details.

6 Astrometry

For the longest possible epoch difference we used the B-band image of Motch et al. (2003) from the year 2000 and compared the position of all objects with the positions in our image from 2008. The objects in the two images are assigned to each other and the change of position is calculated (Fig. 8).

Afterwards the change of position undergoes a Kolmogorov-Smirnov 2-sample test comparing the absolute position changes of the objects to a simulated Rayleigh distribution. The test is performed comparing the cumulative distribution functions (CDF) of the test sample and the data. If the test fails objects lying outside 2σ from the mean of the distribution are excluded. The mean and standard deviation of the distribution are recalculated and the motion of all objects is shifted by that mean to reduce the last remaining systematical errors. This is repeated until the test succeeds. What is left is a sample of Rayleigh distributed background

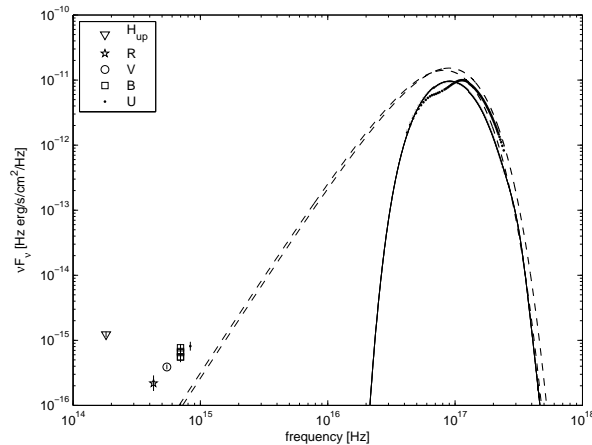


Fig. 7 Optical/UV flux from R to UV magnitudes (our new V-band data point is marked as circle) compared to X-Ray spectra obtained from XMM-Newton EPIC-pn (right) performed in full frame mode with thin filter. The two spectra of RX J0720.4-3125 are taken from orbit 0078 (grey dots) and 0815 (black dots) with effective temperatures of $86.5 \pm 0.4 \text{ eV}$ and $94.6 \pm 0.5 \text{ eV}$, respectively. The solid line marks the best fit model for rev. 0078 (including interstellar extinction), while the dashed lines corresponding to the black bodies for both spectra without any absorption. The broad absorption feature near 300 eV ($\cong 7.25 \cdot 10^{16} \text{ Hz}$) can be seen in the spectrum of revolution 0815 (black dots). The Optical magnitudes are summarized in table 2, the flux in the H band is an upper limit.

stars, without any systematic effects. The standard deviation σ_{Back} of these stars could be seen as total calibration error. Since the NS is much fainter than the background stars, the positional error of its photo-center is relatively large. We added the intrinsic proper motion error $\Delta\mu_{\text{intr}}$ (which is again calculated by the position error in both epochs and

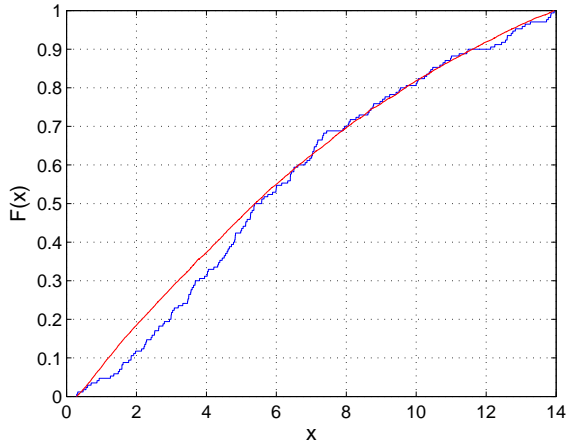


Fig. 9 Cumulative distribution function (CDF) of the Rayleigh distributed background stars in the RX J0720.4-3125 field, compared with the CDF of a synthetic Rayleigh distribution. The comparison shows good agreement, proving that there are no systematical errors left in the calculation.

the epoch difference) of the NS in both epochs to that error, representing the full error of the neutron stars motion as

$$\Delta\mu_{\text{NS}} = \sqrt{(\Delta\mu_{\text{intr}})^2 + (\sigma_{\text{back}})^2}.$$

The mean intrinsic error is already included in σ_{Back} but is larger for the barely visible NS than for the background objects.

We derive a proper motion value

$$\mu_{\alpha} = (-93.2 \pm 5.4) \text{ mas/yr}$$

$$\mu_{\delta} = (48.6 \pm 5.1) \text{ mas/yr}$$

$$\mu = (105.1 \pm 7.4) \text{ mas/yr.}$$

$$\theta = (296.951 \pm 0.0063)^{\circ}$$

This proper motion is consistent with previously published values (Kaplan et al. 2007; Motch et al. 2003). RX J0720.4-3125 changed its position from December 2000 (MJD = 51902 days) to January 2008 (MJD = 54477 days) from

$$\begin{array}{l} \text{MJD} = 51902 \text{ days :} \\ 7^{\text{h}} 20^{\text{m}} 24.976^{\text{s}} \quad -31^{\text{d}} 25' 50.105'' \quad \text{to} \\ \pm 14.15 \text{ mas} \quad \pm 12.82 \text{ mas} \\ \text{MJD} = 54477 \text{ days :} \\ 7^{\text{h}} 20^{\text{m}} 24.926^{\text{s}} \quad -31^{\text{d}} 25' 49.776'' \\ \pm 19.78 \text{ mas} \quad \pm 19.30 \text{ mas,} \end{array}$$

Since the total exposure time in the year 2000 image was longer and the observation wavelength was shorter, our newly reduced position measurement of the year 2000 is more precise and the signal to noise ratio is better.

7 Summary

Taking a deep optical image of RX J0720.4-3125 we were able to determine the V magnitude and updated the position.

Our proper motion ($\mu = 105.1 \pm 7.4$ mas) confirms the measurement obtained by Kaplan et al. (2007) with the HST (107.8 ± 1.2 mas) with a difference of less than 3 mas/yr.

Our V magnitude ($V = 26.81 \pm 0.09$ mag) is compatible with previous observations from Motch et al. (2003) ($B = 26.620 \pm 0.050$ mag) and from (Kulkarni & van Kerkwijk (1998)) ($R = 26.9 \pm 0.3$ mag). These data can be fitted by the emergent spectrum of the photoionized plasma, surrounding the NS (Hambaryan et al. 2009). This scenario would also explain the power-law component of the "optical excess" (Kaplan et al. 2003), which is confirmed by our data.

For further investigations correlated observations in X-ray and the optical/UV are needed to collect enough data to investigate the nature of the flux variations of RX J0720.4-3125 and to understand this isolated neutron star.

We also note, that there are no additional faint, fast moving objects detected in this field (by comparing the year 2000 observations and our image), hence no additional similar NS in this field.

Acknowledgements. The authors would like to thank Frank Haberl, Fred Walter, Andreas Seifahrt and Tristan Röhl for fruitful discussions and improving comments. Furthermore we thank the Staff members of ESO Paranal observatory for their help and assistance carrying out the observations. Based on observations made with ESO Telescopes at the La Silla or Paranal Observatories under programme ID 66.D-0286(A). Moreover we thank Emmanuel Bertin and his team for providing new data reduction software. This research has made use of the VizieR catalogue access tool, CDS, Strasbourg, France. This work was supported in part by DFG grant SFB/Transregio 7 "Gravitational Wave Astronomy". CG acknowledges support by DFG grand under project NE 515/30-1. The work of MMH has been supported by CompStar, a research networking programme of the European Science Foundation (ESF). TOBS acknowledges support from Evangelisches Studienwerk e.V. Villigst.

References

- Appenzeller, I., et al. 1998, *The Messenger*, 94, 1
- Bertin, E. 2006, *Astronomical Data Analysis Software and Systems XV*, 351, 112
- Bertin, E., & Arnouts, S. 1996, *A&AS*, 117, 393
- Bertin, E., Mellier, Y., Radovich, M., Missonnier, G., Didelon, P., & Morin, B. 2002, *Astronomical Data Analysis Software and Systems XI*, 281, 228
- Cutri, R. M., et al. 2003, *The IRSA 2MASS All-Sky Point Source Catalog*, NASA/IPAC Infrared Science Archive. <http://irsa.ipac.caltech.edu/applications/Gator/>,
- de Vries, C. P., Vink, J., Méndez, M., & Verbunt, F. 2004, *A&A*, 415, L31
- Dorman, B., Arnaud, K. A., & Gordon, C. A. 2003, *Bulletin of the American Astronomical Society*, 35, 641
- Haberl, F. 2004, *Advances in Space Research*, 33, 638
- Haberl, F. 2007, *Ap&SS*, 308, 181
- Haberl, F., Turolla, R., de Vries, C. P., Zane, S., Vink, J., Méndez, M., & Verbunt, F. 2006, *A&A*, 451, L17
- Haberl, F., Pietsch, W., Motch, C., & Buckley, D. A. H. 1996, *IAU Circ.*, 6445, 2

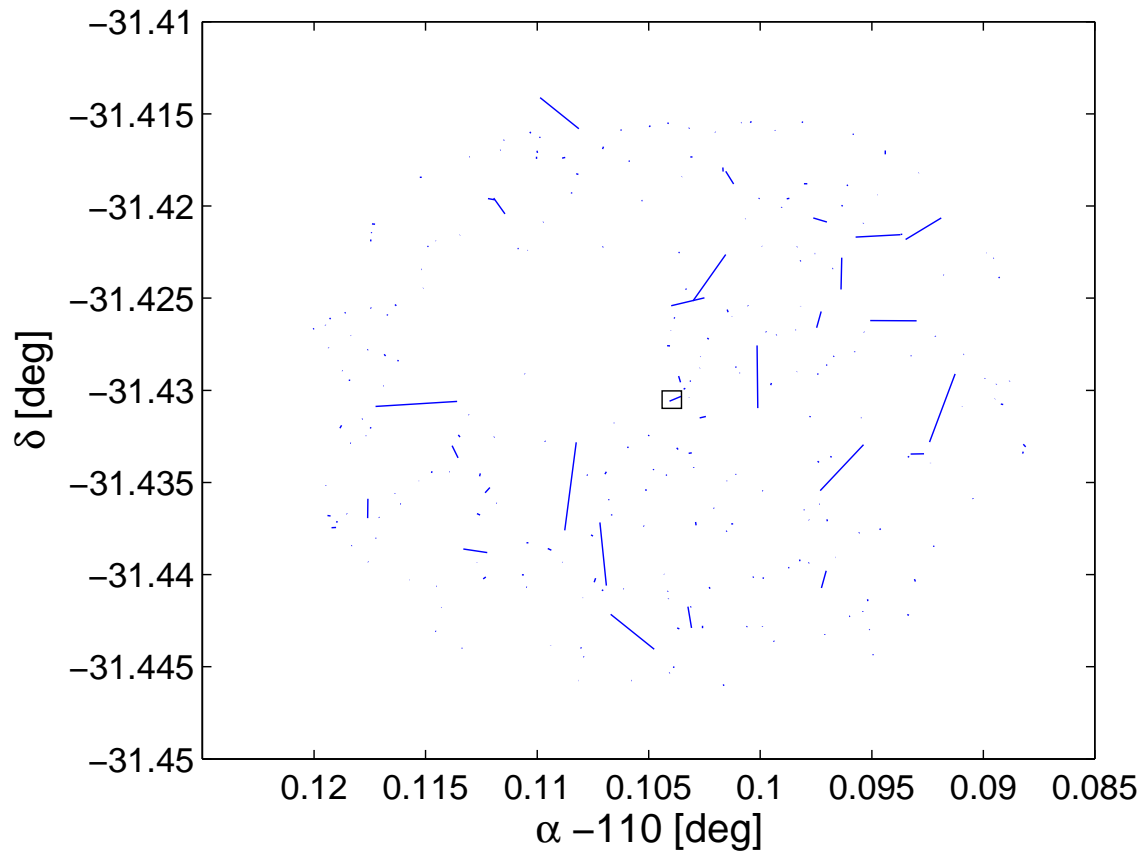


Fig. 8 Detected objects within a radius of 1' around the position of RX J0720.4-3125 . The lines indicate the change of position between the two images of MJD 51902 and MJD 54477 of the objects, scaled up by a factor of 20. While RX J0720.4-3125 (middle) is obviously moving, most of the other objects are almost standing still, demonstrating the high accuracy of the calibration. Other "fast moving" objects are false detections or wrong assignments of objects between the two images.

Haberl, F., Motch, C., Buckley, D. A. H., Zickgraf, F.-J., & Pietsch, W. 1997, *A&A*, 326, 662
 Hambaryan, V., Neuhäuser, R., Haberl, F., Hohle, M. M., & Schwope, A. D. 2009, *A&A*, 497, L9
 Hohle, M. M., Haberl, F., Vink, J., Turolla, R., Hambaryan, V., Zane, S., de Vries, C. P., & Méndez, M. 2009, *A&A*, 498, 811
 Kaplan, D. L., van Kerkwijk, M. H., & Anderson, J. 2002, *ApJ*, 571, 447
 Kaplan, D. L., van Kerkwijk, M. H., & Anderson, J. 2007, *ApJ*, 660, 1428
 Kaplan, D. L., van Kerkwijk, M. H., Marshall, H. L., Jacoby, B. A., Kulkarni, S. R., & Frail, D. A. 2003, *ApJ*, 590, 1008
 Kulkarni, S. R., & van Kerkwijk, M. H. 1998, *ApJ*, 507, L49
 Landolt, A. U. 1992, *AJ*, 104, 340
 Motch, C., & Haberl, F. 1998, *A&A*, 333, L59
 Motch, C., Zavlin, V. E., & Haberl, F. 2003, *A&A*, 408, 323
 Ochsenein, F., Bauer, P., & Marcout, J. 2000, *A&AS*, 143, 23
 Posselt, B., Neuhäuser, R., & Haberl, F. 2009, *A&A*, 496, 533
 Stetson, P. B. 1987, *PASP*, 99, 191
 Trümper, J. E. 2005, *NATO ASIB Proc. 210: The Electromagnetic Spectrum of Neutron Stars*, 117
 Turolla, R., Zane, S., & Drake, J. J. 2004, *ApJ*, 603, 265
 van Kerkwijk, M. H., & Kaplan, D. L. 2007, *Ap&SS*, 308, 191

Voges, W., et al. 1999, *A&A*, 349, 389

Walter, F. M., Wolk, S. J., & Neuhäuser, R. 1996, *Nature*, 379, 233

Zane, S., Turolla, R., & Drake, J. J. 2004, *Advances in Space Research*, 33, 531

Zane, S., Turolla, R., & Page, D. 2007, *Isolated Neutron Stars: from the Surface to the Interior*, Edited by Silvia Zane, Roberto Turolla, and Dany Page. Berlin: Springer, 2007. ISBN: 978-1-4020-5997-1,